

Bonding and Structure of Heavily π -Loaded Complexes

Michael T. Benson,[‡] Jeffrey C. Bryan,[‡] Anthony K. Burrell,[‡] and Thomas R. Cundari*

Department of Chemistry, The University of Memphis, Memphis, Tennessee 38152, and Inorganic and Structural Chemistry Group, CST-3, Los Alamos National Laboratory, Los Alamos, New Mexico 87545

Received October 6, 1994[Ⓢ]

A study of tris(imido) complexes is reported in which X-ray crystallography and molecular orbital calculations are used to probe the bonding in heavily π -loaded transition metal complexes. In this work we focus on Tc-tris(imido) complexes of the form TcX(NR)₃. The bonding in tris(imido) complexes is very sensitive to the nature of the X group. The Tc–N_{imido}–H angle and Tc–N_{imido} bond length are not sensitive enough to X to use in probing the bonding in these complexes. Also, there is no correlation between these two metric parameters. The metric parameter which is the best gauge for changes in electronic structure of the complex is the X–Tc–N_{imido} angle. Subtle variations in X–Tc–N_{imido} as a function of X are accurately reproduced by calculations for an entire series of X ligands from hard ligands to soft metal electrophiles to three-coordinate complexes in which no X ligand is present. Analysis of the trends in X–Tc–N_{imido} as a function of the acid–base properties of X lead to the conclusion that the X ligand exerts its influence on the bonding through the σ framework. The solid-state structures of ReI(NAr)₃ and TcMe(NAr)₃ (Ar = 2,6-diisopropylphenyl) were investigated by X-ray crystallography: ReI(NAr)₃, orthorhombic, *Fdd2*, *a* = 36.874(10) Å, *b* = 39.297(11) Å, *c* = 10.506(2) Å, *V* = 15,223(7) Å³, *Z* = 16; TcMe(NAr)₃, orthorhombic, *Fdd2*, *a* = 37.007(14) Å, *b* = 40.287(13) Å, *c* = 10.607(2) Å, *V* = 15,813(9) Å³, *Z* = 16.

Introduction

Complexes with a multiple bond between a transition metal (TM) and main group element justifiably occupy a position of great importance in inorganic chemistry.¹ These complexes make excellent subjects for study because of the many important reactions they mediate. Imido complexes possess a multiple bond between nitrogen and a transition metal and formally arise from coordination of nitrene, i.e. L_nM(NR).² Much of the early interest in imidos arose from their putative intermediacy in nitrogen fixation and ammoxidation.¹ Imido chemistry has attracted renewed interest for two reasons. First, the imido ligand (NR²⁻) allows stabilization of high formal oxidation states. Second, putting sufficient electron density on the imido N boosts the reactivity of these typically inert ligands.^{1,2a,3} A particularly attractive reaction is the activation of hydrocarbon C–H bonds. Several experimental labs have demonstrated the ability of imidos to effect this reaction, including activation of methane.⁴ Oxo ligands also stabilize high oxidation states and can activate C–H bonds, but the imido has the advantage in that varying the electronic and steric nature of R gives one exquisite control over the properties of the resulting complex. For example, when Ar' = 2,6-C₆H₃Me₂ the complex Tc₂(NAr')₆

has an edge sharing tetrahedral geometry with two bridging imidos.⁵ However, replacement of the *o*-methyl groups with isopropyl groups (Ar = 2,6-C₆H₃-*i*-Pr₂) yields a remarkable ethane-like geometry in Tc₂(NAr)₆.⁶ Much current research revolves around investigating new bonding and reactivity patterns for the versatile imido ligand. Wigley has recently published a review of imidos,^{2a} while computational studies of their bonding and reactivity have been reported by Cundari.⁷

One new strategy for novel imido chemistry involves repeated coordination of imido ligands to a single transition metal center for which Wigley has coined the term π -loading.⁸ Multiple coordination of hard ligands such as NR²⁻ should help to further stabilize high oxidation states. Additionally, coordination of more than one strongly π -bonding ligand will lead to increased competition for metal $d\pi$ –N_{imido} $p\pi$ bonding and hence weakened π bonding. Since many reactions of imidos proceed through cleavage of the MN π bond one can propose that π -loaded poly(imido) complexes may possess greater potential reactivity vs mono(imido) analogues. The Wolczanski^{4a} and Horton^{4b} groups have studied d⁰ bis(imido) complexes of Ta and V, respectively, and demonstrated their ability to activate methane. Cundari has compared methane activation by d⁰, three-coordinate Group IVB bis(amido)imido and Group VB bis(imido)amido complexes.^{7a} The results are inconclusive about the efficacy of π -loading for yielding more potent methane activators, but suggest that further π -loading beyond that in a bis(imido) complex may yield interesting chemistry.

* Address correspondence to this author at the University of Memphis.
[†] The University of Memphis.

[‡] Los Alamos National Laboratory.

[Ⓢ] Abstract published in *Advance ACS Abstracts*, April 15, 1995.

- (1) Nugent, W. A.; Mayer, J. M. *Metal-Ligand Multiple Bonds*; Wiley: New York, 1988.
- (2) (a) Wigley, D. E. *Prog. Inorg. Chem.* **1994**, *42*, 239. (b) Nugent, W. A.; Haymore, B. L. *Coord. Chem. Rev.* **1980**, *31*, 123. (c) Cenini, S.; LaMonica, G. *Inorg. Chim. Acta* **1976**, *18*, 279. (d) Dehnicke, K.; Strahle, J. *Angew. Chem., Int. Ed. Engl.* **1981**, *20*, 413.
- (3) Bryan, J. C.; Burrell, A. K.; Miller, M. M.; Smith, W. H.; Burns, C. J.; Sattelberger, A. P. *Polyhedron* **1993**, *12*, 1769.
- (4) (a) Schaller, C. P.; Wolczanski, P. T. *Inorg. Chem.* **1993**, *32*, 131. (b) de With, J.; Horton, A. D. *Angew. Chem., Int. Ed. Engl.* **1993**, *32*, 903. (c) Cummins, C. C.; Baxter, S. M.; Wolczanski, P. T. *J. Am. Chem. Soc.* **1988**, *110*, 8731. (d) Walsh, P. J.; Hollander, F. J.; Bergman, R. G. *J. Am. Chem. Soc.* **1988**, *110*, 8729. (e) Bennett, J. L.; Wolczanski, P. T. *J. Am. Chem. Soc.* **1994**, *116*, 2179.

- (5) Burrell, A. K.; Clark, D. L.; Gordon, P. L.; Sattelberger, A. P.; Bryan, J. C. *J. Am. Chem. Soc.* **1994**, *116*, 3813.
- (6) Burrell, A. K.; Bryan, J. C. *Angew. Chem., Int. Ed. Engl.* **1993**, *32*, 94.
- (7) (a) Cundari, T. R. *Organometallics* **1994**, *13*, 2987. (b) Cundari, T. R. *J. Am. Chem. Soc.* **1992**, *114*, 7879. (c) Cundari, T. R. *J. Am. Chem. Soc.* **1992**, *114*, 10557. (d) Cundari, T. R. *Intern. J. Quantum Chem., Proc. Sanibel Symp.* **1992**, *26*, 793. (e) Cundari, T. R. *Organometallics* **1993**, *12*, 1998. (f) Cundari, T. R. *Organometallics* **1993**, *12*, 4971. (g) Benson, M. T.; Cundari, T. R.; Li, Y.; Strohecker, L. A. *Intern. J. Quantum Chem., Proc. Sanibel Symp.* **1994**, *28*, 181.
- (8) Chao, Y. W.; Rodgers, P. M.; Wigley, D. E.; Alexander, S. J.; Rheingold, A. L. *J. Am. Chem. Soc.* **1991**, *113*, 6326.

The logical extension of the π -loading strategy is coordination of three imidos to a single metal.⁹ To date no one has isolated a three-coordinate, d^0 tris(imido) complex although Wigley has isolated a PMe_3 adduct of $\text{W}(\text{NAr})_3$ and shown it to be capable of activating the C–H bonds of terminal alkynes.¹⁰ Three-coordinate, d^2 tris(imido) complexes have been isolated. Schrock et al. have structurally characterized $\text{Os}(\text{NAr})_3$ ¹¹ and the PPN^+ salt of $[\text{Re}(\text{NAr})_3]^-$.¹² The Tc analogue of the anion has been studied, but displays higher reactivity and was not structurally characterized.⁵ Four-coordinate complexes of the form $\text{XM}(\text{NR})_3$ where X is typically a univalent ligand are well-known. The majority of these complexes incorporate metals from the Mn triad. Wilkinson and co-workers have published extensively on the synthesis, reactivity, and structure of Re–tris(imido)¹³ and Mn–tris(imido) complexes.¹⁴ The Bryan group has studied the chemistry of Tc–tris(imido) complexes.^{5,6,15}

The goal of this research is to combine theory and experiment to probe the consequences of heavily π -loading a single transition metal center. Technetium is an important radiometal and many Tc radiopharmaceuticals contain the TcO moiety. It should be possible to replace the oxo ligand with an isovalent NR ligand and obtain greater control over properties such as biodistribution through manipulation of the R group.¹⁶ Also, d^0 $\text{M}(\text{NR})_3$ complexes would seem too reactive to be amenable to experimental investigation. Studying $\text{XM}(\text{NR})$ complexes allows, in essence, investigation of “trapped” tris(imido) transients of potential interest as methane-activating complexes. How well trapped tris(imido) complexes model the evanescent tris(imido) is best probed through a combination of theory and experiment.

Experimental Section

1. X-ray Crystal Structure Determination for $\text{ReI}(\text{NAr})_3$ and $\text{TcMe}(\text{NAr})_3$. $\text{ReI}(\text{NAr})_3$ ⁵ and $\text{TcMe}(\text{NAr})_3$ ³ were prepared as previously described. Suitable single crystals were grown by slow evaporation of THF ($\text{ReI}(\text{NAr})_3$) and Et_2O ($\text{TcMe}(\text{NAr})_3$). $\text{TcMe}(\text{NAr})_3$ formed as a dark green cube measuring $0.15 \times 0.18 \times 0.20$ mm, and was

Table 1. Summary of Crystallographic Data

complex	$\text{ReI}(\text{NAr})_3 \cdot 1/2 \text{THF}$	$\text{TcMe}(\text{NAr})_3 \cdot 1/2 \text{Et}_2\text{O}$
chem formula	$\text{C}_{38}\text{H}_{55}\text{IN}_3\text{O}_{1/2}\text{Re}$	$\text{C}_{39}\text{H}_{59}\text{N}_3\text{O}_{1/2}\text{Tc}$
<i>a</i> , Å	36.874(10)	37.007(14)
<i>b</i> , Å	39.297(11)	40.287(13)
<i>c</i> , Å	10.506(2)	10.607(2)
<i>V</i> , Å ³	15,223	15,813
<i>Z</i>	16	16
fw	875.0	675.8
space group	<i>Fdd2</i> (No. 43)	<i>Fdd2</i> (No. 43)
<i>T</i> , °C	–70	22
λ , Å	0.710 73	0.710 73
ρ_{calcd} , g cm ^{–3}	1.53	1.13
μ , cm ^{–1}	40.3	3.9
<i>R</i> ^a	0.024	0.059
<i>R</i> _w ^b	0.029	0.067

$$^a R = \sum ||F_o| - |F_c|| / \sum |F_o|. \quad ^b R_w = [\sum w(|F_o| - |F_c|)^2 / \sum w(F_o)^2]^{1/2}.$$

Table 2. Selected Bond Lengths (Å) and Angles (deg) (M = Re, Tc; X = I, CH₃)

	$\text{ReI}(\text{NAr})_3$	$\text{TcMe}(\text{NAr})_3$
Re–I	2.644(1)	
Tc–C(1)		2.136(17)
M–N(1)	1.770(7)	1.738(11)
M–N(2)	1.767(6)	1.749(13)
M–N(3)	1.765(6)	1.743(10)
X–M–N(1)	106.7(2)	101.8(6)
X–M–N(2)	105.9(2)	102.9(6)
X–M–N(3)	105.4(2)	101.4(6)
N(1)–M–N(2)	113.8(3)	116.6(6)
N(1)–M–N(3)	112.1(3)	115.7(5)
N(2)–M–N(3)	112.2(3)	115.0(5)
M–N(1)–C(10)	165.7(6)	167.0(11)
M–N(2)–C(22)	169.9(6)	163.9(10)
M–N(3)–C(34)	167.5(5)	168.0(9)

sealed inside a glass capillary. $\text{ReI}(\text{NAr})_3$ formed a dark red cube measuring $0.24 \times 0.26 \times 0.23$ mm, and was mounted on a glass fiber. Preliminary photographic examination and data collection were performed on a Siemens R3m/V diffractometer with graphite-monochromated Mo $K\alpha$ radiation. Cell constants and an orientation matrix were obtained by least-squares refinement, using the setting angles of at least 25 reflections. Good crystal quality was also suggested by measuring ω scans of several intense reflections and by examining axial photographs. Intensity data were obtained using ω scans. A total of 7020 reflections ($4 \leq 2\theta \leq 50^\circ$, $-h, \pm k, l$) were collected on $\text{ReI}(\text{NAr})_3$, and 5255 reflections ($2 \leq 2\theta \leq 45^\circ$, $h, k, \pm l$) on $\text{TcMe}(\text{NAr})_3$. The data were scaled for linear decay. A semiempirical absorption correction (XEMP) based on the average relative intensity curve of azimuthal scan data was applied for $\text{ReI}(\text{NAr})_3$. No absorption correction was applied to the data for $\text{TcMe}(\text{NAr})_3$ because of its low absorption coefficient and good crystal shape. The data for $\text{ReI}(\text{NAr})_3$ were averaged over *mmm* symmetry ($R_{\text{int}} = 2.0\%$). Redundant data were not collected for $\text{TcMe}(\text{NAr})_3$. The structures were solved using standard heavy atom methods and refined with full-matrix least-squares methods. All non-hydrogen atoms were refined anisotropically. Hydrogen atom positions were calculated (C–H = 0.96 Å) and added to the structure factor calculations without refinement. Only the 3257 independent reflections with $F > 3\sigma_F$ were used in the refinement of $\text{ReI}(\text{NAr})_3$, and the 1949 reflections with $F > 4\sigma_F$ were used in the refinement of $\text{TcMe}(\text{NAr})_3$. All calculations were performed using SHELXTL PLUS programs provided by Siemens Analytical. Crystallographic data are given in Table 1, selected bond lengths and angles in Table 2, and selected atomic coordinates in Tables 3 and 4. Complete tabulations of crystallographic data, bond lengths and angles, atomic coordinates, thermal parameters, and completely labeled ball and stick diagrams are available as supplementary material.

2. Computational Methods. Our main approach to the challenges of computational TM chemistry entails design, testing and use of effective core potentials.^{7,17} Great savings in time, memory and disk space are effected by replacing the many core electrons, and the basis

- (9) Several tetrakis(imido) complexes have been made, but they tend to interact strongly with cationic counterions.^{2a} In $[\text{Re}(\text{N}-t\text{-Bu})_4][\text{Li}(\text{TMEDA})]$ the solvated Li^+ counterion interacts strongly with two of the “imido” ligand.^{9a} The complex $[\text{Li}_2\text{W}(\text{N}-t\text{-Bu})_4]$ is a dimer in the solid-state and the Li^+ counterions coordinate to “imido” ligands in neighboring $[\text{W}(\text{N}-t\text{-Bu})_4]^{2-}$ units.^{9a} A monomeric, neutral tetrakis(imido) $[\text{Os}(\text{N}-t\text{-Bu})_4]$ has very recently been structurally characterized by gas-phase electron diffraction.^{9b} (a) Danopoulos, A. A.; Wilkinson, G.; Hussain, B.; Hursthouse, M. B. *J. Chem. Soc.* **1989**, 896. (b) Rankin, D. W.; Robertson, H. E.; Danopoulos, A. A.; Lyne, P. D.; Mingos, D. M. P.; Wilkinson, G. W. *J. Chem. Soc., Dalton Trans.* **1994**, 1563.
- (10) Wigley, D. E.; Morrison, D. Department of Chemistry, University of Arizona, personal communication.
- (11) (a) Anhaus, J. T.; Kee, T. P.; Schofield, M. H.; Schrock, R. R. *J. Am. Chem. Soc.* **1990**, *112*, 1642. (b) Schofield, M. H.; Kee, T. P.; Anhaus, J. T.; Schrock, R. R.; Johnson, K. H.; Davis, W. M. *Inorg. Chem.* **1991**, *30*, 3595.
- (12) (a) Williams, D. S.; Anhaus, J. T.; Schofield, M. H.; Schrock, R. R.; Davis, W. M. *J. Am. Chem. Soc.* **1991**, *113*, 5480. (b) Williams, D. S.; Schrock, R. R. *Organometallics* **1993**, *12*, 1148.
- (13) (a) Saboonchian, V.; Danopoulos, A. A.; Gutierrez, A.; Wilkinson, G.; Williams, D. J. *Polyhedron* **1991**, *10*, 2241. (b) Danopoulos, A. A.; Longley, C. J.; Wilkinson, G.; Hussain, B.; Hursthouse, M. B. *Polyhedron* **1989**, *8*, 2657.
- (14) (a) Danopoulos, A. A.; Wilkinson, G.; Sweet, T.; Hursthouse, M. B. *J. Chem. Soc., Chem. Comm.* **1993**, 495. (b) Danopoulos, A. A.; Wilkinson, G.; Sweet, T. K. N.; Hursthouse, M. B. *J. Chem. Soc., Dalton* **1994**, 1037.
- (15) Burrell, A. K.; Bryan, J. C. *Organometallics* **1992**, *11*, 3501.
- (16) (a) Nicholson, T.; Cook, J.; Davison, A.; Jones, A. G. *Inorg. Chim. Acta* **1994**, *218*, 97. (b) Archer, C. M.; Dilworth, J. R.; Jobanputra, P.; Thompson, R. M.; McPartlin, M.; Povey, D. C.; Smith, G. W.; Kelly, J. D. *Polyhedron* **1990**, *12*, 1497.

Table 3. Selected Coordinates ($\times 10^4$) for $\text{ReI}(\text{NAr})_3$

	<i>x</i>	<i>y</i>	<i>z</i>	U_{eq}^a
Re	10708(1)	14062(1)	100000	226(1)
I	5813(1)	10122(1)	111003(11)	387(2)
N(1)	9402(17)	14486(17)	83870(65)	279(19)
N(2)	10659(16)	17931(16)	108565(63)	281(19)
N(3)	14864(14)	11877(15)	101637(66)	258(17)
C(10)	9229(20)	14487(21)	70772(79)	282(22)
C(22)	10983(20)	21172(19)	113507(76)	288(22)
C(34)	18349(19)	10887(18)	103363(71)	253(15)

^a Equivalent isotropic U_{eq} defined as one third of the trace of the orthogonalized U_{ij} tensor and given in units of $\text{\AA}^2 \times 10^3$.

Table 4. Selected Coordinates ($\times 10^4$) for $\text{TcMe}(\text{NAr})_3$

	<i>x</i>	<i>y</i>	<i>z</i>	U_{eq}^a
Tc	8629(1)	8975(1)	0	50(1)
N(1)	8617(3)	9336(3)	-899(12)	58(4)
N(2)	8472(3)	9006(3)	1551(13)	66(5)
N(3)	9012(3)	8728(2)	-196(11)	55(4)
C(1)	8225(4)	8679(4)	-893(18)	81(6)
C(10)	8642(4)	9655(3)	-1375(13)	56(4)
C(22)	8447(4)	9006(3)	2863(13)	56(4)
C(34)	9355(3)	8594(3)	-336(12)	50(4)

^a Equivalent isotropic U_{eq} defined as one third of the trace of the orthogonalized U_{ij} tensor and given in units of $\text{\AA}^2 \times 10^3$.

functions describing them, with a small number of potentials. Relativistic effects are incorporated into ECP derivation; transition metal ECPs are generated from all-electron, Dirac-Fock calculations, and thus include Darwin and mass velocity effects, while spin-orbit coupling is averaged out in potential generation.¹⁸

Calculations employ the parallel quantum chemistry program GAMESS.¹⁹ For this research the iPSC/860 (Oak Ridge), SP-1 (Cornell Theory Center), and parallel IBM cluster (Memphis) were used as platforms. Effective core potentials (ECPs) and valence basis sets are used for all heavy atoms and the -31G basis set for H.¹⁸ ECPs replace the innermost core orbitals for TMs and all core orbitals for main-group (MG) elements. Thus, the *ns*, *np*, *nd*, (*n* + 1)*s* and (*n* + 1)*p* are treated explicitly for the d-block; for the main-group *ns* and *np* are treated explicitly. Transition metal valence basis sets are quadruple and triple ζ for *sp* and *d* shells, respectively, while main-group elements have a double- ζ valence basis. Basis sets for heavy MG elements are augmented with a *d* polarization function. Unless stated otherwise, geometries are optimized at the restricted Hartree-Fock (RHF) level for closed-shell singlets. Bond lengths and angles for TM complexes are typically predicted to within 1–3% of experiment using the present scheme involving complexes in a variety of geometries and formal oxidation states and with metals from the entire transition series.^{7,17} Vibrational frequencies are calculated at stationary points to identify them as minima (zero imaginary frequencies) or transition states (one imaginary frequency).

Results and Discussion

1. Molecular Structures of $\text{ReI}(\text{NAr})_3$ and $\text{TcMe}(\text{NAr})_3$

In order to add to our experimental structural database of $\text{MX}(\text{NR})_3$ complexes, we determined the solid-state structures of $\text{ReI}(\text{NAr})_3$ ⁵ and $\text{TcMe}(\text{NAr})_3$ ³ (*Ar* = 2,6-diisopropylphenyl) by single-crystal X-ray diffraction. Crystallographic parameters and other information related to data collection and solution

(17) Cundari, T. R.; Gordon, M. S. *Coord. Chem. Rev.*, in press.

(18) Krauss, M.; Stevens, W. J.; Basch, H.; Jasien, P. G. *Can. J. Chem.* **1992**, *70*, 612.

(19) (a) Schmidt, M. W.; Baldrige, K. K.; Boatz, J. A.; Jensen, J. H.; Koseki, S.; Matsunaga, N. M.; Gordon, M. S.; Nguyen, K. A.; Su, S.; Windus, T. L.; Elbert, S. T. *J. Comput. Chem.* **1993**, *14*, 1347. (b) Applications of parallel GAMESS can be found in: Baldrige, K. K.; Boatz, J. A.; Cundari, T. R.; Gordon, M. S.; Jensen, J. H.; Matsunaga, N. M.; Schmidt, M. L.; Windus, T. L. In *Parallel Computing in Computational Chemistry*; Mattson, T. G., Ed.; American Chemical Society Symposium Series: American Chemical Society: Washington, DC, in press.

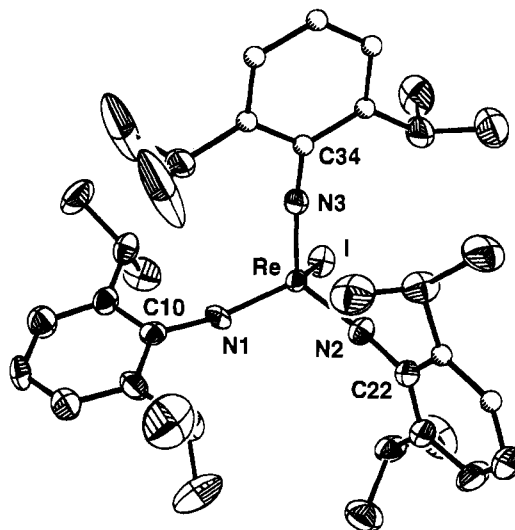


Figure 1. ORTEP drawing (50% probability ellipsoids) of $\text{ReI}(\text{NAr})_3$. Isotropically refined atoms are represented as shaded spheres. Hydrogen atoms are omitted for clarity.

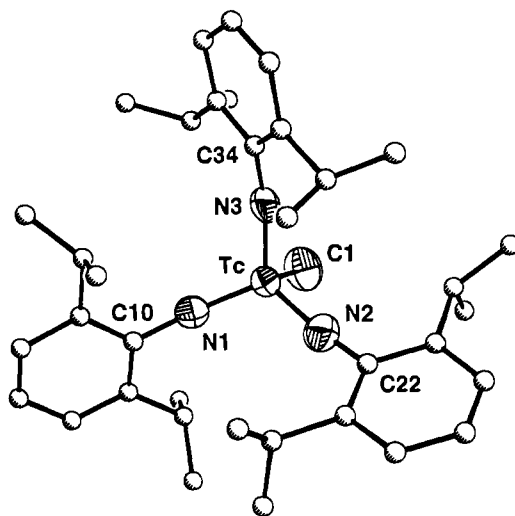
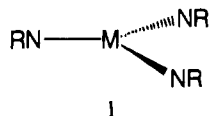


Figure 2. ORTEP drawing (50% probability ellipsoids) of $\text{TcMe}(\text{NAr})_3$. Isotropically refined atoms are represented as shaded spheres. Hydrogen atoms are omitted for clarity.

are summarized in Table 1, selected bond lengths and angles are given in Table 2, and ORTEP diagrams are presented in Figures 1 ($\text{ReI}(\text{NAr})_3$) and 2 ($\text{TcMe}(\text{NAr})_3$). Both compounds exhibit approximate tetrahedral coordination environments about the metal, and short metal–nitrogen multiple bond lengths (1.738(11)–1.770(7) \AA).^{1,2a} These structures are very similar to previously determined structures of closely related complexes $\text{TcI}(\text{NAr})_3$ ³ and $\text{Tc}(\eta^1\text{-Cp})(\text{NAr})_3$ ¹⁵. The only noteworthy difference between $\text{ReI}(\text{NAr})_3$ and $\text{TcI}(\text{NAr})_3$ is that the M–I bond distance is 0.01 \AA shorter in the Re structure. On the basis of periodic trends, the opposite should be true. The major difference between $\text{TcMe}(\text{NAr})_3$ and $\text{Tc}(\eta^1\text{-Cp})(\text{NAr})_3$ is that the C–Tc– N_{imido} angles tend to be smaller (and the N_{imido} –Tc– N_{imido} angles correspondingly larger) for $\text{TcMe}(\text{NAr})_3$. This may simply be a reflection of the lower steric demands of methyl vs $\eta^1\text{-Cp}$. The structures of $\text{ReI}(\text{NAr})_3$ and $\text{TcMe}(\text{NAr})_3$ are discussed relative to other known $\text{MX}(\text{NR})_3$ complexes below.

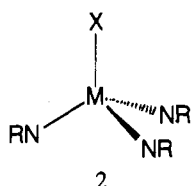
2. Geometries of Tris(imido) Complexes. a. Three-Coordinate Complexes. Structurally characterized three-coordinate tris(imido) complexes possess d^2 electronic configurations and trigonal planar coordination geometries.^{11,12} The bonding in tris(imido)



complexes, including the structural preference for trigonal planarity, has been studied in detail using X α calculations.¹¹ Calculations using ECP methods have also been reported for Os(NH)₃ and [Re(NH)₃]⁻ as part of a survey of the bonding in TM imido complexes.^{7b} These d² model complexes possess trigonal planar minimum energy geometries^{7b} as found experimentally.^{11,12}

Given their importance in this work, geometry optimizations on [Tc(NH)₃] transients were carried out. Calculated data are summarized in Table 5. The PPN⁺ salt of [Tc(NAr)₃]⁻ slowly decomposes in solution thus hindering structural characterization.⁵ Calculations were carried out on the Tc-tris(imido) cation (d⁰), radical (d¹), and anion (d²) to assess the effect of d orbital occupation. Calculated Tc-N_{imido} bond lengths increase in the order cation < radical < anion as expected given the decrease in the Tc formal oxidation state. Calculated Tc-N_{imido} bond lengths are consistent with characterized Tc-tris(imido) complexes. The d² anion is trigonal planar (C_{3h}) consistent with experimental data for Os(NAr)₃ and [Re(NAr)₃]⁻. The calculated Tc-N_{imido} bond length of 1.77 Å in [Tc(NH)₃]⁻ is equal to that for the Re analogue as expected given their similar covalent radii. The d⁰ tris(imido) cation is pyramidal. The d² complexes remain planar because even though they are formally 20-electron complexes two electrons remain in a ligand-based nonbonding MO in a planar geometry.¹¹ The d⁰ systems are 18-electron complexes and thus there is no electronic impetus for remaining planar and the complex pyramidalizes to minimize competition for Tc d π -N_{imido} p π bonding. It is of great interest, therefore, that the d¹ [Tc(NH)₃] radical is trigonal planar. Clearly, putting one electron in the metal based MO is more than enough to tip the balance toward a planar geometry in order not to have an electron count greater than 18 around the metal.

b. Four-Coordinate Complexes. Roughly two dozen pseudotetrahedral XM(NR)₃ complexes have been structurally characterized, 2. The majority of these complexes incorporate



metals from the Mn triad. To our knowledge, the only examples of non-Group VIIB tris(imido) complexes are those reported by Wigley and co-workers, [WCl(NAr)₃Cl]⁻ and W(PMe₃)(NAr)₃.^{8,10,21} The ligand X is typically a univalent ligand such as an alkoxide or halide. Bryan et al. have structurally characterized complexes where X is a soft metal electrophile such as [Au(PPh₃)₃]⁺, [Hg(Tc(NAr)₃)₃]⁺, and *Tc(NAr)₃,^{5,6} and also alkyl ligands¹⁵ (X = Me, η^1 -Cp) which can be considered intermediate between soft electrophiles and hard nucleophiles.

(20) Nugent, W. A.; Harlow, R. L.; McKinney, R. J. *J. Am. Chem. Soc.* **1979**, *101*, 7265.

(21) Oxotris(imido)osmium(VIII) complexes have been synthesized and their vibrational spectra characterized, but no structural studies, to our knowledge, have been reported. Chong, A. O.; Oshima, K.; Sharpless, K. B. *J. Am. Chem. Soc.* **1979**, *99*, 3420. A tris(imido) of Nb is known although there is bonding of Li⁺ to the "imido" nitrogens in [Li(THF)₂]₂[Nb(NMe₃)₃(*n*-Bu)]. Smith, D. P.; Allen, K. D.; Carducci, M. D.; Wigley, D. E. *Inorg. Chem.* **1992**, *31*, 1319.

Table 5. ECP Calculated Metric Data for XTc(NH)₃ Complexes^{a,b}

complex	X-Tc-N _{imido}	Tc-N _{imido}	Tc-N _{imido} -H
d ² -[Tc(NH) ₃] ⁻	90.0	1.770	124.4
d ¹ -[Tc(NH) ₃] [•]	90.0	1.740	127.6
Tc(AuPH ₃)(NH) ₃	96.1	1.744	125.2
Tc(SiH ₃)(NH) ₃	96.8	1.737	125.4
Hg(Tc(NH) ₃) ₂	96.9	1.738	126.7
*TcH(NH) ₃	98.9	1.733	123.5
[Tc(NH) ₃] ₂	99.6	1.734	122.5
*Tc(CF ₃)(NH) ₃	99.7	1.730	123.5
*TcMe(NH) ₃	100.5	1.733	123.1
[Tc(P(OH) ₃)(NH) ₃] ⁺	100.6	1.722	128.9
<i>Tc</i> (η^1 -Cp)(NH) ₃	101.1 ± 0.6	1.732 ± 0.002	122.5 ± 0.4
*Tc(CN)(NH) ₃	101.2	1.729	122.7
*Tc(CCl ₃)(NH) ₃	101.5	1.730	122.3
[Tc(PH ₃)(NH) ₃] ⁺	101.7	1.727	130.0
<i>Tc</i> (SCN)(NH) ₃	102.9 ± 3.3	1.729 ± 0.007	123.5 ± 1.7
*Tc(SH)(NH) ₃	103.0 ± 3.7	1.730 ± 0.006	122.3 ± 1.5
[Tc(CO)(NH) ₃]	103.3	1.728	131.0
*TcI(NH) ₃	103.8	1.729	122.6
[Tc(NH ₃)(NH) ₃] ⁺	103.8	1.723	129.1
*Tc(NH ₂)(NH) ₃	104.0 ± 3.7	1.730 ± 0.005	122.5 ± 2.0
*TcBr(NH) ₃	104.6	1.728	122.3
<i>Tc</i> (ONO)(NH) ₃	104.7 ± 2.0	1.726 ± 0.003	122.5 ± 0.7
[Tc(NCMe)(NH) ₃] ⁺	104.8	1.724	127.4
*TcCl(NH) ₃	105.0	1.727	122.1
Tc(NCS)(NH) ₃	105.1	1.727	122.2
*Tc(OH)(NH) ₃	105.4 ± 2.4	1.727 ± 0.002	122.6 ± 0.8
[TcS(NH) ₃] ⁻	106.1	1.750	116.8
*TcF(NH) ₃	106.2	1.724	123.1
[TcN(NH) ₃] ²⁻	107.7	1.879	104.0
[Tc(NH) ₃] ⁺ [BF ₄]	108.3	1.729	121.4
d ⁰ -[Tc(NH) ₃] ⁺	108.5	1.726	132.9
[TcO(NH) ₃] ⁻	110.1	1.778	117.3

^a Bond lengths and bond angles were determined at the RHF level as described in Computational Methods. For complexes without 3-fold symmetry (in italics) a range is given for Tc-N_{imido} bond lengths, and Tc-N_{imido}-H and X-Tc-N_{imido} angles. ^b 3-fold symmetry was assumed in four of the larger complexes (Tc(AuPH₃)(NH)₃, [Tc(P(OH)₃)(NH)₃]⁺, [Tc(NCMe)(NH)₃]⁺, and [Tc(NH)₃]⁺[BF₄]). All other complexes were completely geometry optimized and are minima on their respective potential energy surfaces. ^c These complexes were used in calibration of the ECT parameterization of the X-Tc-N_{imido} angle, see eq 1.

Thus, this research provides an interesting assortment of X groups to assess their effect on the tris(imido) functionality.

A previous extensive survey of imido complexes clearly shows the current ECP/valence basis set scheme (VBS) to be capable of predicting M-L (L is a generic ligand) bond lengths and L-M-L bond angles to within 1-3%.¹⁷ It has been a general observation that the ability to model transition metal complexes at the simplest (i.e., Hartree-Fock) level of theory diminishes as one goes to the right in the first transition series. A good example of this is provided by Mn-tris(imido) complexes such as MnCl(N-*t*-Bu)₃ recently characterized by Wilkinson et al.,¹⁴ which we modeled using MnCl(NMe)₃ and MnCl(NH)₃, both of which give very poor agreement with experimental data: Mn-N = 1.87 Å (H), 1.84 Å (Me), 1.66 Å (*t*-Bu, experimental^{14a}); Mn-Cl = 2.21 Å (H), 2.24 Å (Me), 2.22 Å (*t*-Bu, experimental^{14a}); Cl-Mn-N = 135° (H), 126° (Me), 107 ± 1° (*t*-Bu, experimental^{14a}); N-Mn-N = 76° (H), 88° (Me), 111 ± 1° (*t*-Bu, experimental^{14a}). Using a correlated wavefunction (Møller-Plesset second order perturbation theory²²) for geometry optimization greatly improves the agreement between experiment and theory: Mn-N = 1.56 Å; Mn-Cl = 2.09 Å; Cl-Mn-N = 105°; N-Mn-N = 113° for MnCl(NH)₃ at the MP2 level. The angles about Mn are nearly within the limits of experimental uncertainty. A result of including

(22) Møller, C.; Plesset, M. S. *Phys. Rev.* **1934**, *46*, 618.

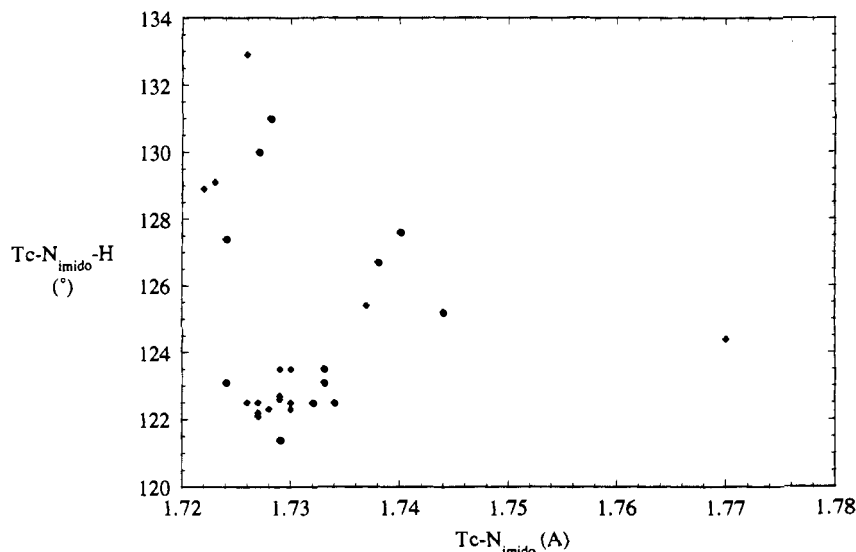


Figure 3. Plot of calculated $\text{Tc-N}_{\text{imido}}\text{-H}$ angle (deg) vs $\text{Tc-N}_{\text{imido}}$ bond length (Å) for the complexes in Table 5; complexes with multiply bonded X ligands ($\text{X} = \text{N}^{3-}, \text{O}^{2-}, \text{S}^{2-}$) are excluded.

correlation is a noticeable shortening of the Mn–ligand bond lengths so that they are roughly 6% shorter than reported for $\text{ClMn}(\text{N-}i\text{-Bu})_3$; thus, $\text{Mn-N}_{\text{imido}}$ is in much improved agreement with experiment, but still roughly 0.1 Å shorter than reported by Wilkinson et al.^{14a} In a previous survey of multiply bonded complexes it was also seen that MP2 tended to overcorrect for differences seen between experiment and RHF geometries.^{7g,23} The Mn calculations are valuable because they serve to emphasize the fact that regardless of the flexibility of the ECP/VBS scheme, the wavefunction used must be suitable to describe the system of interest. An accurate description of Mn–imido complexes will most likely necessitate more sophisticated multiconfigurational methods.

One can envision three metric parameters with which to probe the bonding in tris(imido) complexes: $\text{Tc-N}_{\text{imido}}$ distance, $\text{X-Tc-N}_{\text{imido}}$ angle, and $\text{Tc-N}_{\text{imido}}\text{-H}$ angle. The $\text{N}_{\text{imido}}\text{-Tc-N}_{\text{imido}}$ and $\text{X-Tc-N}_{\text{imido}}$ angles are related and the former approaches 120° as the latter approaches 90° for a complex with 3-fold symmetry. Tc- and Re–tris(imido) complexes are appropriately described at the Hartree–Fock level and thus the present calculations should accurately predict their structure.¹⁷ Experimentally characterized $\text{Tc-N}_{\text{imido}}$ bond lengths in tris(imido) complexes range from ≈ 1.72 to 1.76 Å while $\text{Re-N}_{\text{imido}}$ bond lengths span a somewhat greater range, $1.68\text{--}1.76$ Å. Calculated $\text{Tc-N}_{\text{imido}}$ bond lengths for tris(imido) models are 1.74 ± 0.03 Å for the examples in Table 5. The only complexes with $\text{M-N}_{\text{imido}}$ bond lengths significantly higher than the average are those in which X is itself a strong multiple bonding ligand like an oxo ($\text{Tc-N}_{\text{imido}} = 1.778$ Å for $[\text{TcO}(\text{NH})_3]^-$) and N^{3-} ($\text{Tc-N}_{\text{imido}} = 1.879$ Å for $[\text{TcN}(\text{NH})_3]^{2-}$). Sulfido does not effectively compete with imido for $d\pi\text{-}p\pi$ bonding; $\text{Tc-N}_{\text{imido}} = 1.750$ Å in $[\text{TcS}(\text{NH})_3]^-$. Removal of multiply bonded ligands from the structural database (Table 5) yields even less variation in the $\text{Tc-N}_{\text{imido}}$ bond length; the average $\text{Tc-N}_{\text{imido}}$ bond length is now 1.73 ± 0.01 Å. In either case, calculated $\text{Tc-N}_{\text{imido}}$ bond lengths are consistent with structurally characterized Tc tris(imido) complexes.^{3,5,6,15} Given the narrow range of $\text{Tc-N}_{\text{imido}}$ bond lengths, this metric parameter is not likely to be a sufficiently sensitive probe of the bonding in tris(imido) complexes.

There has been much discussion in the literature about the correlation between $\text{M-N}_{\text{imido}}$ bond lengths and $\text{M-N}_{\text{imido}}\text{-R}$ angles and its implication for the nature of the metal–imido bond.^{1,2,7b} Bent and linear imido coordination are often taken

to represent metal–nitrogen double (3) and triple (4) bonds,



respectively. However, closer inspection of the experimental and computational literature of imido complexes suggests that trends in $\text{M-N}_{\text{imido}}$ bond lengths and $\text{M-N}_{\text{imido}}\text{-R}$ bond angles are not so clear cut. For example, Parkin et al.^{24a} have characterized a $\text{Ta}^{\text{V}}\text{-N}_{\text{imido}}$ complex for which $\text{Ta-N}_{\text{imido}} = 1.831(10)$ Å, substantially longer than reported for other linearly coordinated Ta^{V} imido complexes. The average $\text{Ta}^{\text{V}}\text{-N}_{\text{imido}} = 1.77 \pm 0.01$ Å for the three four-coordinate complexes in the compendium by Nugent and Mayer.¹ However, Gray et al. have characterized a four-coordinate, $\text{Ta}^{\text{V}}\text{-N}_{\text{imido}}$ complex with an extremely bent coordination mode ($\text{Ta-N}_{\text{imido}}\text{-C} = 145.7(6)^\circ$), but with a $\text{Ta-N}_{\text{imido}}$ bond length ($1.779(8)$ Å) equal to linearly coordinated analogues.^{24b} This recent X-ray crystallographic work highlights the dangers in using structural data (in particular $\text{M-N}_{\text{imido}}\text{-R}$ angles) as the sole inference for the nature of the metal–imido bond. Detailed computations^{7b} show the metal–imido bond to be more complicated than a single resonance structure description; there are eight dominant resonance structures to describe the metal–imido linkage, some of which do not correspond to those previously discussed in the literature.^{7b} In Figure 3 calculated $\text{Tc-N}_{\text{imido}}\text{-H}$ angles are plotted vs $\text{Tc-N}_{\text{imido}}$ bond lengths for Tc–tris(imido) models using the data in Table 5. Even by excluding multiply bonded ligands ($\text{X} = \text{nitrido, oxo, sulfido}$) as done in Figure 3, it is obvious that there is no correlation between the two metric parameters. Most Tc–

(23) A comparison of RHF and MP2 geometries for $\text{TcI}(\text{NH})_3$ with the X-ray structure³ of $\text{TcI}(\text{NAr})_3$ also illustrates this observation. The $\text{Tc-N}_{\text{imido}}$ bonds go from 0.03 Å shorter than experiment at the RHF level to 0.03 Å too long at the MP2 level. Calculated $\text{I-Tc-N}_{\text{imido}}$ and $\text{N}_{\text{imido}}\text{-Tc-N}_{\text{imido}}$ angles are 2° less and greater, respectively, than in $\text{TcI}(\text{NAr})_3$ at the RHF levels; at the MP2 level the situation is reversed with the former being 2° greater than $\text{I-Tc-N}_{\text{imido}}$ and the latter being 2° less than $\text{N}_{\text{imido}}\text{-Tc-N}_{\text{imido}}$ in the X-ray structure. However, unlike Mn complexes, the magnitude of the changes in geometries is small, supporting the appropriateness of a Hartree–Fock description for Tc complexes.

(24) (a) Parkin, G.; Van Asselt, A.; Leahy, D. J.; Winnery, L.; Hua, N. G.; Quan, R.; Henling, L. M.; Schaefer, W. P.; Santarsiero, B. D.; Bercaw, J. E. *Inorg. Chem.* **1992**, *31*, 82. (b) Gray, S. D.; Smith, D. P.; Bruck, M. A.; Wigley, D. E. *J. Am. Chem. Soc.* **1992**, *114*, 5462.

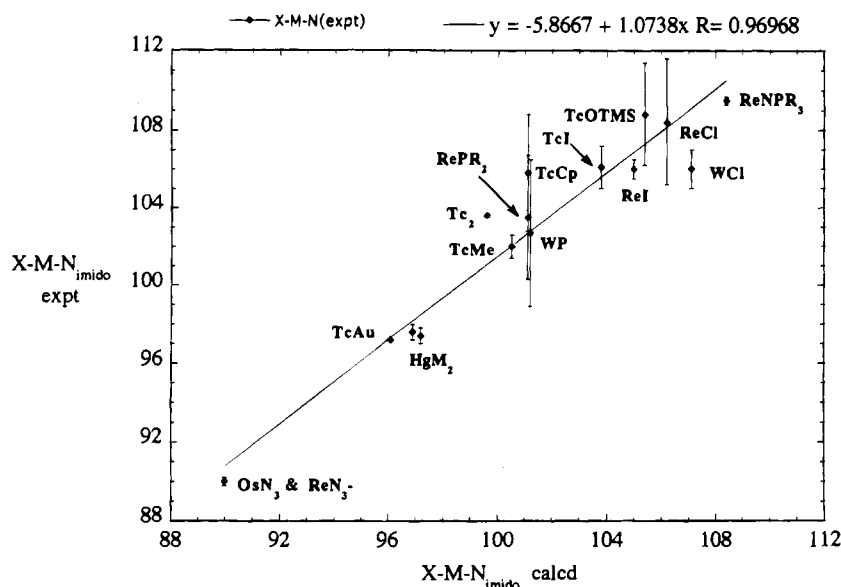


Figure 4. Plot of calculated $X-M-N_{\text{imido}}$ (deg) for $XM(NH)_3$ vs those experimentally determined for $XM(NR)_3$. $OsN_3 = Os(NAr)_3$, $ReN_3^- = [Re(NAr)_3]^-$, $TcAu = (NAr)_3TcAuPPh_3$, $HgM_2 = Hg(Tc(NAr)_3)_2$ and its Re analogue, $Tc_2 = [Tc(NAr)_3]_2$, $TcMe = TcMe(NAr)_3$, $WP = W(PMe_3)(NAr)_3$, $RePR_2 = Re(PPh_2)(N-t-Bu)_3$, $TcI = Tc(NAr)_3$, $ReI = ReI(NAr)_3$, $TcOTMS = Tc(OTMS)(NAr)_3$, $ReCl = ReCl(N-t-Bu)_3$, $ReNPR_3 = Re(NAr)_3(NPPH_3)$, $TcCp = Tc(\eta^1-Cp)(NAr)_3$, and $WCl = [WCl(NAr)_3]^-$. Error bars indicate the range of $X-Tc-N_{\text{imido}}$ for complexes in which there is not a crystallographic 3-fold axis.

$N_{\text{imido}}-H$ bond angles lie between 120 and 130° despite the softness of this mode. As with $Tc-N_{\text{imido}}$ distances, $Tc-N_{\text{imido}}-H$ angles are not sufficiently sensitive for probing the bonding in these complexes.

The final metric parameter of interest in the analysis of tris(imido) complexes is $X-M-N_{\text{imido}}$ angle. It is imperative that the computational model be able to accurately reproduce this angle. Shown in Figure 4 is a plot of calculated vs experimental $X-M-N_{\text{imido}}$ angles for 16 complexes: $Os(NAr)_3$,¹¹ $[Re(NAr)_3]^-$,¹² $(NAr)_3TcAuPPh_3$,⁵ $Hg(M(NAr)_3)_2$ ($M = Tc$,⁵ Re ¹²), $[Tc(NAr)_3]_2$,⁶ $TcMe(NAr)_3$, $W(PMe_3)(NAr)_3$,¹⁰ $Re(PPh_2)(N-t-Bu)_3$,^{13a} $MI(NAr)_3$ ($M = Tc$,³ Re), $Tc(OTMS)(NAr)_3$,³ $ReCl(N-t-Bu)_3$,^{13b} $Re(NAr)_3(NPPH_3)$,²⁵ $Tc(\eta^1-Cp)(NAr)_3$,¹⁵ and $[WCl(NAr)_3]^-$.⁸ Computational models were generated by replacement of bulky aryl and alkyl groups and silyl groups with H atoms, converting the complexes listed above to $Os(NH)_3$, $[Re(NH)_3]^-$, $(NH)_3TcAuPH_3$, $Hg(M(NH)_3)_2$, $[Tc(NH)_3]_2$, $TcMe(NH)_3$, $W(PH_3)(NH)_3$, $Re(PH_2)(NH)_3$, $MI(NH)_3$, $Tc(OH)(NH)_3$, $ReCl(NH)_3$, $Re(NH)_3(NPH_3)$, $Tc(\eta^1-Cp)(NH)_3$, and $[WCl(NH)_3]^-$. Mn-tris(imido) complexes were not included since a Hartree-Fock wave function is not appropriate (*vide supra*). In only a few cases does the experimental span of $X-M-N_{\text{imido}}$ angles not fall on or near the best-fit line; see Figure 4. The complex in which there is the greatest difference is the Tc-tris(imido) dimer. In $[Tc(NH)_3]_2$ the $Tc-Tc-N_{\text{imido}}$ angle is 99.6° , or 4° less than that measured for $[Tc(NAr)_3]_2$. It is possible that the larger angle observed experimentally is due to steric repulsions between the two large $[Tc(NAr)_3]$ units. However, despite the modifications needed to make the computations tractable there is an excellent correlation between calculated and experimental $X-M-N_{\text{imido}}$ angles. As in previous studies of multiply bonded transition metal complexes,^{17,26} ECP methods in conjunction with RHF wave functions are able to accurately predict structural features such as bond lengths but even more subtle trends in geometric factors and their response to the chemical environment.

3. Bonding and Structure in Tris(imido) Complexes.

From the above discussion it is apparent that the metric parameters of greatest interest in probing the bonding in $MX(NR)_3$ are the angles about the metal. In characterized $MX(NR)_3$ complexes $X-M-N_{\text{imido}}$ ranges from 97.2° ($Tc(AuPPh_3)(NAr)_3$) to 109.5° ($Re(NPPH_3)(NAr)_3$). If one includes three-coordinate complexes then the $X-Tc-N_{\text{imido}}$ angles range down to 90° (X is the approximate 3-fold axis). As seen in Figure 4 the calculations are very capable of accurately predicting trends in $X-Tc-N_{\text{imido}}$ as a function of X . Upon inspection of the data in Table 5 several trends emerge. First, $X-Tc-N_{\text{imido}}$ increases in the order $I < Br < Cl < F$. Second, sulfido ($S-Tc-N_{\text{imido}} = 106.1^\circ$) and thiol ($S-Tc-N_{\text{imido}} = 103.0^\circ$) complexes have smaller $X-Tc-N_{\text{imido}}$ angles than their oxygen counterparts ($O-Tc-N_{\text{imido}} = 110.1^\circ$ and 105.4° for oxo and hydroxy, respectively). One ligand which seems to fall outside the norm is CF_3 , a group one normally considers to be electron withdrawing; the $C-Tc-N_{\text{imido}}$ angle in the CF_3 complex (99.7°) is smaller than that in the methyl analogue (100.5°). Perhaps the π -donor ability of fluoride is manifesting itself in the presence of a d^0 metal. Third, relatively electroneutral and electropositive ligands like silyl and the soft metal electrophiles show the smallest $X-Tc-N_{\text{imido}}$ angles.

Calculations on three-coordinate Tc-tris(imido) complexes, **1**, are very interesting and provide an entry point into understanding the bonding in the four-coordinate complexes, **2**. Since $d^0-[Tc(NH)_3]^+$ is pyramidal while the radical and anion are trigonal planar, one can propose that as the $Tc(NH)_3$ unit in $X-Tc(NH)_3$ becomes increasingly cationic the tris(imido) moiety should become increasingly pyramidalized. Thus, as the $X-Tc(NH)_3$ bond becomes increasingly polarized in a $X^{\delta-}-[Tc(NH)_3]^{\delta+}$ fashion the $X-Tc-N_{\text{imido}}$ angle should increase and approach values closer to tetrahedral as in $[Tc(NH)_3]^+$ (the angle between the C_3 axis and the $Tc-N_{\text{imido}}$ bond is 108.5°). Conversely, as the $X-Tc-N_{\text{imido}}$ angle approaches 90° one can infer that the Tc-tris(imido) moiety is becoming less cationic in nature.

In order to better understand how X affects the bonding in $X-Tc(NH)_3$ a correlation between $X-Tc-N_{\text{imido}}$ and Drago's acid-base parameters was investigated.²⁷ Drago et al. have

(25) Roesky, H. W.; Hesse, D.; Noltemeyer, M.; Sheldrick, G. M. *Chem. Ber.* **1991**, *124*, 757.

(26) Cundari, T. R.; Critchlow, S. C.; Conry, R. R.; Spaltenstein, E. V.; Hall, K. A.; Tahmassebi, S.; Mayer, J. M. *Organometallics* **1994**, *13*, 322.

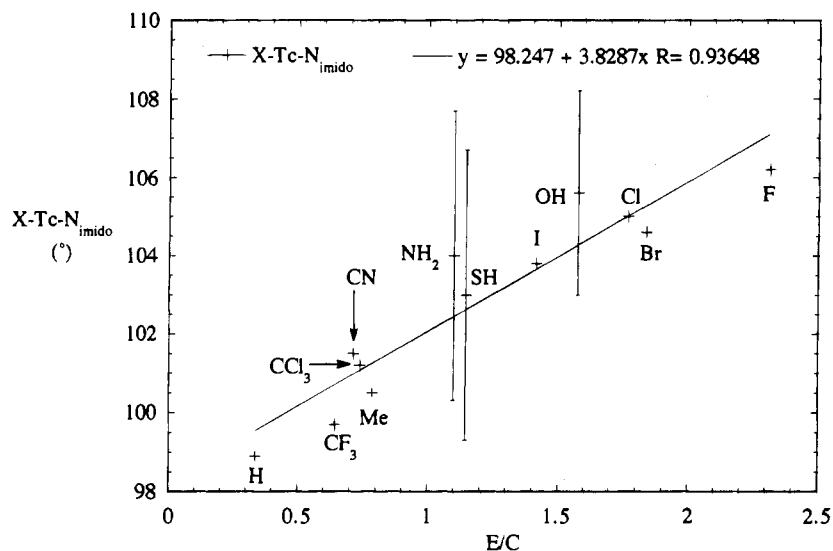


Figure 5. Plot of calculated X-Tc-N_{imido} (deg) in XTc(NH)₃ vs Drago's E/C ratio for X = H, CF₃, Me, CN, CCl₃, SH, NH₂, I, Br, Cl, OH, and F.²⁷ For X = NH₂, OH, and SH there is no 3-fold rotation axis and error bars indicate range of X-Tc-N_{imido} angles.

reported parameters for describing metal-ligand bonds in organometallics.²⁷ This ECT method decomposes the M-X bond energy into electrostatic (*E*), covalent (*C*), and electron transfer (*T*) contributions. There are twelve XTc(NH)₃ complexes studied with ECP methods (see Table 5) for which X is in the Drago database. Plotting *E*, *C*, or *T* vs the X-Tc-N_{imido} angle reveals no linear correlation between these quantities. There is a good linear correlation between calculated X-Tc-N_{imido} and the *E/C* ratio, see Figure 5. As *E/C* increases for a given X, the importance of electrostatics in its bonding with metal centers increases.²⁷ It is interesting that ligands most deviant from the best-fit line in Figure 5 (X = F, OH, NH₂) are ligands where one might predict π -bonding to be most significant in the Tc-X bond. Tc(NH₂)(NH)₃ and Tc(OH)(NH)₃ are not 3-fold symmetric, and thus X-Tc-N_{imido} angles span a range of values which in both cases fall on the best-fit line, Figure 5. Of course, this is not the case for TcF(NH)₃. However, the correlation in Figure 5 is good despite the deviations noted, and shows that X-Tc-N_{imido} increases as the *E/C* ratio increases. The ECT parameters describe X as the anionic end of a polarized M-X bond so that the correlation in Figure 5 supports the above contention that X-Tc-N_{imido} increases in response to a metal-ligand bond which is increasingly polarized X ^{δ^-} -[Tc(NH)₃] ^{δ^+} .

One can fit X-Tc-N_{imido} to an equation such as eq 1. Parameters *E_x*, *C_x* and *T_x* are found in a database²⁷ while X-Tc-N_{imido} is determined by quantum calculation (Table 5). Using ECT parameters (X = H, Me, OH, SH, NH₂, CN, CF₃,

$$X-Tc-N_{imido} = E_x k_1 + C_x k_2 + T_x k_3 \quad (1)$$

CCl₃, Cl, Br, I, F) and calculated X-Tc-N_{imido} (relative to H-Tc-N_{imido}) the best-fit is obtained when *k*₁ = 0.9021, *k*₂ = -0.7133, and *k*₃ = -0.5385.²⁸ These constants can then be used to predict other systems for which ECT parameters are known and for which quantum calculations have yet to be performed. There are six additional X groups in the ECT

Table 6. ECP Calculated Metric Data for Additional XTc(NH)₃ Complexes^{a,b}

complex	X-Tc-N _{imido}	Tc-N _{imido}	Tc-N _{imido} -H
<i>TcEt</i> (NH) ₃	100.3 ± 0.3	1.734 ± 0.001	123.5 ± 0.5
<i>Tc</i> (<i>C</i> (O)Me)(NH) ₃	100.7 ± 2.3	1.734 ± 0.004	124.2 ± 0.7
<i>Tc</i> (CH=CH ₂)(NH) ₃	101.0 ± 0.5	1.732 ± 0.001	122.5 ± 0.8
[Tc(CCH)(NH) ₃]	102.4	1.730	122.3
<i>Tc</i> (SMe)(NH) ₃	102.7 ± 2.9	1.731 ± 0.005	122.2 ± 1.2
<i>Tc</i> (OMe)(NH) ₃	105.2 ± 1.5	1.728 ± 0.002	122.3 ± 0.5

^a Bond lengths and bond angles were determined at the RHF level as described in Computational Methods. For complexes without perfect 3-fold symmetry (in italics) a range is given for Tc-N_{imido} bond lengths, and Tc-N_{imido}-H and X-Tc-N_{imido} angles. ^b These six additional TcX(NH)₃ complexes were calculated to test the predictive capacity of the ECT analysis. All complexes were completely geometry optimized and are minima on their respective potential energy surfaces.

database²⁸ (X = Et, C(O)CH₃, vinyl, C≡CH, OMe and SMe) which are of a size to be amenable to quantum calculation, Table 6. The X-Tc-N_{imido} angles (relative to H-Tc-N_{imido}) estimated from the ECT fit (eq 1) are consistent with those subsequently determined by ECP methods, Figure 6. The acid-base parameters are derived such that only σ -bonding contributions to the M-X bond energy are considered. Deviations arise when π -bonding is significant.²⁷ The correspondence between ECP and ECT analyses of X-Tc-N_{imido} angles further supports the hypothesis that X influences the bonding in the Tc-tris(imido) complex through the σ framework.

Summary and Conclusions

In summary, a study of tris(imido) complexes is reported in which X-ray crystallography and computational methods are combined to probe the bonding in heavily π -loaded transition metal complexes. We focused on Tc-tris(imido) complexes of the form TcX(NR)₃ because of the rich database of structurally characterized complexes incorporating chemically distinct X groups. Several interesting conclusions resulting from this work are summarized below.

(1) The bonding in the tris(imido) complex is very sensitive to the X group. It was found that the Tc-N_{imido}-H angle and Tc-N_{imido} bond length are not sensitive enough to X to be of any use in probing the bonding in these complexes. Furthermore, there is no correlation between these two metric parameters. This last observation is consistent with the rising volume

(27) Drago, R. S.; Wong, N. M.; Ferris, D. C. *J. Am. Chem. Soc.* **1992**, *114*, 91.

(28) The fitting procedure is described in: Drago, R. S. *Applications of Electrostatic-Covalent Models in Chemistry*; Surfside Scientific: Gainesville, FL, 1994. The constants *k_n* yield a X-Tc-N_{imido} bond angle relative to that in the hydride (H-Tc-N_{imido} = 98.9°); hence the ECT parameters used in fitting Equation 1 are also relative to *E_x*, *C_x*, and *T_x* for X = H.

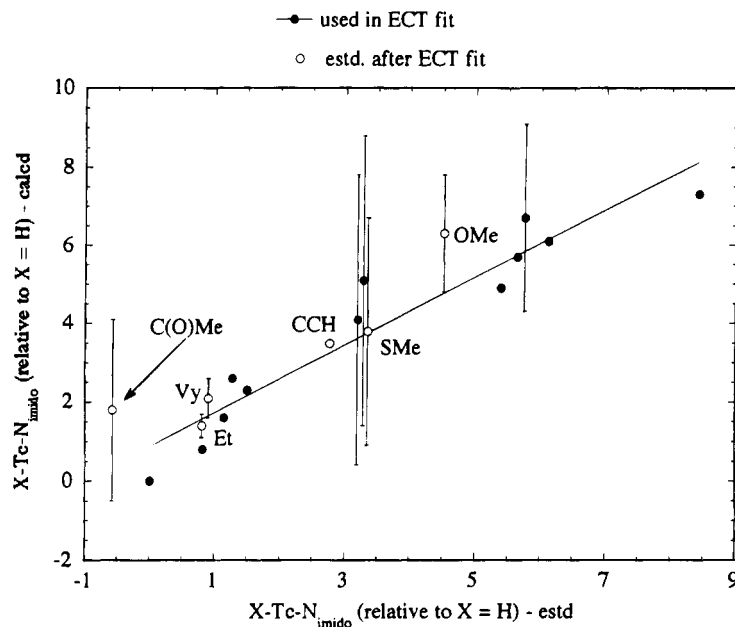


Figure 6. The $X\text{-Tc-N}_{\text{imido}}$ angles (deg) calculated using ECP methods are compared with those estimated from ECT analysis. Filled points are X groups used in obtaining the best fit to eq 1. Open points are complexes ($X = \text{Et}$, $\text{C}(\text{O})\text{CH}_3$, vinyl, $\text{C}\equiv\text{CH}$, OMe and SMe) first estimated using the ECT fit and then subsequently calculated using ECP methods. Error bars indicate range of angles for complexes without 3-fold symmetry.

of experimental and computational data which show that inferring details about the nature of the metal-imido bond from correlations between $M\text{-N}_{\text{imido}}\text{-R}$ and $M\text{-N}_{\text{imido}}$ is tenuous.

(2) The metric parameter which is the best gauge for changes in electronic structure of the complex is the $X\text{-Tc-N}_{\text{imido}}$ angle. Structurally characterized complexes show a wide range ($\approx 20^\circ$) in $X\text{-Tc-N}_{\text{imido}}$; subtle experimental variations are accurately reproduced by calculations for an entire series of X ligands from hard nucleophiles to soft metal electrophiles to three-coordinate complexes in which no X ligand is present. This further demonstrates the utility of computational methods which can predict subtle structural features and hence shed light on the interactions which give rise to them.

(3) Trends in $X\text{-Tc-N}_{\text{imido}}$ as a function of X lead to the interesting conclusion that X exerts the majority of its influence on the bonding in $\text{MX}(\text{NR})_3$ through the σ framework. Correlation of changes in $X\text{-Tc-N}_{\text{imido}}$ angles with acid-base (ECT) parameters supports this conclusion. Furthermore, it was possible to use the acid-base database, which contains many common ligands, to reliably predict structural changes found to be in good agreement with those subsequently determined with quantum chemical methods. There are two advantages to using the ECT scheme. First, once the method has been calibrated the analysis is very quick and can be used to screen large families of complexes. One can focus on X ligands predicted to yield the most interesting changes in bonding and structure. Second, the approach affords simple interpretations sometimes absent in sophisticated calculations and hence a clearer picture of the chemistry giving rise to observed trends.

Acknowledgment. T.R.C. would like to acknowledge the donors of the Petroleum Research Fund (administered by the American Chemical Society), the Air Force Office of Scientific Research, the National Science Foundation (through their support of Cornell Theory Center), and the U.S. Department of Energy (Grant DE-FG05-94ER14460 from the Division of Chemical Sciences, Office of Basic Energy Sciences, Office of Energy Research) for support of ECP studies at Memphis. We also acknowledge Oak Ridge National Labs (ORNL) for allowing access to the iPSC/860 through participation in the Joint Institute for Computational Science (a consortium between Memphis, ORNL, Tennessee-Knoxville, and Vanderbilt to support supercomputing in Tennessee). This research was carried out while T.R.C. was a visiting scientist at Los Alamos National Lab (LANL) and was supported by Laboratory Directed Research and Development funds. M.T.B. acknowledges a Graduate Research Assistantship from the LANL. We thank Prof. R. J. Butcher (Howard University) for assistance with the structure of $\text{ReI}(\text{NAr})_3$. Helpful discussions with Prof. R. S. Drago (Florida), Dr. D. R. Wheeler (Sandia Labs), and Prof. J. M. Mayer (Washington) are gratefully acknowledged.

Supplementary Material Available: Complete tabulations of crystal data bond lengths and angles, atomic coordinates, thermal parameters, and completely labeled diagrams for $\text{ReI}(\text{NAr})_3$ and $\text{TcMe}(\text{NAr})_3$ (18 pages). This material is contained in many libraries on microfiche, immediately follows this article in the microfilm version of the journal, and can be ordered from the ACS; see any current masthead page for ordering information.

IC9411559